

FIGURE 3. Selected (A) oblique and (B) sagittal slices of the liver-spleen SPECT. The original coronal slices were slightly reoriented to display better the origin of the anomalous splenic tissue at the lower pole of the spleen. With SPECT no further image enhancement is necessary.

noninvasiveness, relatively low price, sensitivity and specificity make scintigraphy well suited for screening purposes.

REFERENCES

1. Putschar WGJ, Manion WC. Splenic-gonadal fusion. *Am J Path* 1956;32:15-35.
2. Toriello HV. Splenogonadal fusion-limb defect. In: Buyse ML, ed. *Birth defects encyclopedia*. Dover, MA: Blackwell Scientific Publications; 1990:1582.
3. Pauli RM, Greenlaw A. Limb deficiency and splenogonadal fusion. *Am J Med Genetics* 1982;13:81-90.
4. Wejman J. Splenogonadal fusion. A case report. *Patol Pol* 1993; 44:233-235.
5. Miceli AB. Splenogonadal fusion: a rare cause of a scrotal mass. *Br J Urol* 1994; 74:250.
6. Guarin U, Dimitrieva Z, Ashley SJ. Splenogonadal fusion—a rare congenital anomaly demonstrated by ^{99m}Tc -sulphur colloid imaging: case report. *J Nucl Med* 1975;16: 922-924.
7. Wood TW, Magelson N. Urological accessory splenic tissue. *J Urol* 1986;137:1219-1220.
8. Azar GB, Awwad JT, Mufarrj IK. Accessory spleen presenting as adnexal mass. *Acta Obstet Gynecol Scand* 1993;72:587-588.
9. Emmett JM, Dreyfuss ML. Accessory spleen in the scrotum. *Ann Surg* 1943;117:754-759.
10. Watson RJ, Major MC. Splenogonadal fusion. *Surgery* 1968;63:853-858.
11. Halvorsen JF, Stray O. Splenogonadal fusion. *Acta Paediatr Scand* 1978;67:379-381.
12. Andrews RA, Copeland DD, Fried FA. Splenogonadal fusion. *J Urol* 1985;133: 1052-1053.

Copper-62-ATSM: A New Hypoxia Imaging Agent with High Membrane Permeability and Low Redox Potential

Yasuhisa Fujibayashi, Hideyuki Taniuchi, Yoshiharu Yonekura, Hiroshi Ohtani, Junji Konishi and Akira Yokoyama
Departments of Radiopharmaceutical Chemistry and Biomedical Imaging and Biomedical Imaging Research Center, Fukui Medical School, Fukui; Departments of Genetic Biochemistry, Nuclear Medicine and Radiopharmaceutical Chemistry, Faculty of Pharmaceutical Sciences, School of Medicine, Kyoto University, Kyoto; and The First Department of Internal Medicine, Fukushima Medical College, Fukushima, Japan

An ideal hypoxia imaging agent should have high membrane permeability for easy access to intracellular mitochondria and low redox potential to confer stability in normal tissue, but it should be able to be reduced by mitochondria with abnormally high electron concentrations in hypoxic cells. In this context, nitroimidazole residues are not considered to be essential. In this study, Cu(II)-diacetyl-bis(*N*⁴-methylthiosemicarbazone) (Cu-ATSM), a ^{62}Cu -bisthiosemicarbazone complex, with high membrane permeability and low redox potential, was evaluated as a possible hypoxia imaging agent, using electron spin resonance spectrometry and the Langendorff isolated perfused rat heart model as well as rat heart left anterior descending occlusion model. **Methods:** Nonradioactive Cu-ATSM was incubated with rat mitochondria, after which reduction of Cu(II) to Cu(I) was measured with electron spin resonance. As a model of hypoxic mitochondria, rotenone (Complex I inhibitor)-treated mitochondria

were used. **Results:** In this study, Cu-ATSM was reduced by hypoxic but not by normal mitochondria. **Conclusion:** Thus, retention of ^{62}Cu -ATSM was studied serially in perfused rat hearts under conditions of normoxia (95% O₂ + 5% CO₂), hypoxia (95% N₂ + 5% CO₂) and reoxygenation (95% O₂ + 5% CO₂). In normoxia and reoxygenation, ^{62}Cu -ATSM injected as a single bolus showed low retention (23.77% and 22.80%, respectively) 15 min after injection, but retention was increased markedly under hypoxic conditions (81.10%). Also, in the in vivo left anterior descending occluded rat heart model, ^{62}Cu -ATSM retention was inversely correlated with accumulation of ^{201}Tl , a relative myocardial blood flow marker.

Key Words: copper-62-ATSM; hypoxia; mitochondria

J Nucl Med 1997; 38:1155-1160

Hypoxic tissue is important for detection of ischemia in the brain, heart and other tissues, as well as tumors. Nitroimidazole compounds, originally developed as radiosensitizing agents (1), are of great interest because of their selective accumulation in

Received Feb. 2, 1996; revision accepted Jul. 8, 1996.

For correspondence or reprints contact: Yasuhisa Fujibayashi, PhD, Dept. of Genetic Biochemistry, Faculty of Pharmaceutical Sciences, Kyoto University, Kyoto, 606, Japan.

hypoxic tumors (2) as well as ischemic tissues (3). Based on these considerations, various groups have attempted nitroimidazole-based drug design of hypoxia imaging agents labeled with ^{18}F (4), ^{123}I (5,6), $^{99\text{m}}\text{Tc}$ (7,8), etc. However, nitroimidazole itself has very low lipophilicity (9). For use as radiosensitizing agents, interest has moved to more hydrophilic nitroimidazole compounds to reduce neurotoxicity in the central nervous system (9). Tissue extraction of radiolabeled nitroimidazole compounds based on radiosensitizing agents has been very low, and rather long periods were required to obtain acceptable tissue accumulation.

Recently, methods for lipophilicity-based drug design of nitroimidazole compounds have been developed, and improved retention in hypoxic tissue has been reported (10–12). In normal cells, the redox states of the components of the electron transport chain of mitochondria are rather oxidized. Under these conditions, radiolabeled nitroimidazoles cannot be reduced and so are returned to the systemic circulation. In areas of hypoxia, i.e., areas in which electron flow is disturbed by oxygen depletion, radiolabeled nitroimidazoles undergo bioreduction, and the radionuclides are deposited (13). Nitroimidazole compounds are believed to be enzymatically reduced (14) and have high affinity for the nitroreductase enzyme xanthine oxidase (7). Xanthine oxidase is activated under electron- as well as NADH-rich conditions such as hypoxia, and its substrate, xanthine, is known to be produced in ischemic tissues (15) as a degradation product of ATP (16).

We have developed a new type of generator system, eluting ^{62}Cu as glycine complex under physiological conditions (17). Using this Cu-glycine eluate, Cu-bisthiosemicarbazone complexes (Cu-BTS), such as Cu(II)-pyruvadehyde-bis(N^4 -methylthiosemicarbazone) (Cu-PTSM) injectate could be easily prepared by simple mixing with BTS solution without further purification. This generator system is currently in clinical use in combination with the perfusion agent PTSM (18) as well as the plasma imaging agent HSA-BTS (19). In fundamental studies, it was found that Cu-PTSM could be reduced easily by the electron transport system of mitochondria, and this reduction was considered to be a retention mechanism of Cu-PTSM in the brain (20). The redox potential of Cu-PTSM is higher than that of NADH (21), and the reduction of Cu-PTSM by mitochondria was NADH-dependent (22). Interestingly, some Cu-BTS complexes with lower redox potential also showed high membrane permeability including the blood-brain barrier but were not retained in the brain or the heart (23), probably because they could not be reduced by normal mitochondria. If such Cu-BTS complexes can be reduced by abnormally reduced mitochondria, like nitroimidazole compounds, they will become better candidates for hypoxia imaging agents. In fact, some $^{99\text{m}}\text{Tc}$ -BnAO complexes have been reported to show plausible characteristics as hypoxia markers, although the actual retention mechanism is still unknown (24).

In this study, the Cu-BTS complex with low redox potential Cu-ATSM was selected (structure shown in Fig. 1), and its basic ability as a hypoxia imaging agent was evaluated.

MATERIALS AND METHODS

Cu-ATSM and Cu-PTSM were synthesized according to the method of Gingas et al. (25), and chemical purity of each complex was confirmed by elementary analysis and mass spectrometry. [^{62}Zn]ZnCl₂ was a gift from Nihon Medi-Physics Co. Ltd., Japan. Copper-62 was obtained with a $^{62}\text{Zn}/^{62}\text{Cu}$ generator system, originally developed in our laboratory (17). Thallium-201-chloride was also a gift from Nihon Medi-Physics Co. Ltd., Japan. All other chemicals used were of analytical grade.

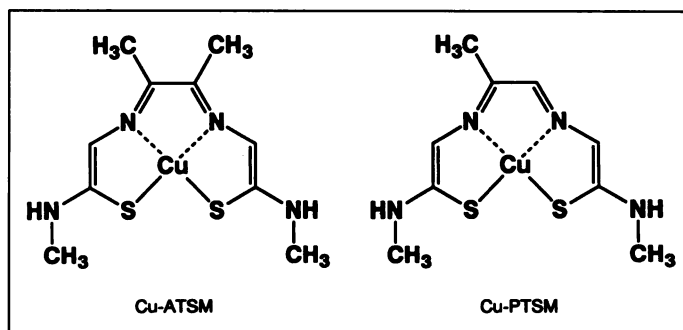


FIGURE 1. Structures of Cu-BTS complexes.

Isolation of Mouse Brain Mitochondria

Mouse brain mitochondria were prepared by the previously reported method (22). Male ddY mice (20–25 g body weight) were killed by decapitation. The mouse brain was homogenized immediately in isolation medium (0.15 g of wet tissue/ml) with a Potter-Elvehjem type homogenizer. The homogenate was centrifuged at $1000 \times g$ for 5 min at 4°C , after which the supernatant (S1) was centrifuged at $10,000 \times g$ for 10 min at 4°C . The supernatant was removed, and the precipitate was resuspended in isolation medium (crude mitochondrial fraction). The volume of the crude mitochondrial fraction was adjusted to the initial value of the brain homogenate volume. The isolation medium contained 0.25 M sucrose and 10 mM succinate buffered at pH 7.4 with 10 mM HEPES (26).

Preparation of Submitochondrial Particles (SMP)

SMP were prepared according to the method of Williams et al. (27). Male ddY mice (20–25 g body weight) were killed by decapitation. The brain was immediately homogenized in H-medium [200 mM D-mannitol, 70 mM sucrose, 0.05% (w/v) bovine serum albumin buffered to pH 7.4 with 2.5 mM HEPES], then the mitochondrial fraction was isolated as described above. The mitochondrial precipitate was resuspended in 2 ml of digitonin solution (12 mg/ml H-medium) and digested for 20 min at 4°C . After digestion, 12 ml of isolation medium was added, and the mixture was centrifuged at $10,000 \times g$ for 10 min at 4°C . The precipitate was resuspended in distilled water to about 30 ml and centrifuged at $10,000 \times g$ for 15 min at 4°C . After centrifugation, the precipitate was resuspended in approximately 2.5 ml of isolation medium and sonicated for 90 s (15 s \times 6 times) (Sonicator, W-220F, Heatsystem-Ultrasonics, Inc.) at 4°C . The resultant SMP suspension was adjusted to 10 mg of protein/ml. Preparation of SMP was confirmed by measuring the enzyme activities of monoamine oxidase (28), succinate dehydrogenase (29) and malate dehydrogenase (30) as marker enzymes.

In Vitro Metabolism Studies with Electron Spin

Resonance Spectrometry

Inhibition of Electron Transport Chain. A 5-ml aliquot of the mitochondrial preparation was mixed with 0.1 μl of rotenone solution (0.5 mg/ml ethanol) and 0.9 ml of isolation medium. A 1.8-ml aliquot of the mixture was mixed with 200 μl of Cu-ATSM solution (0.2 mM) and incubated at 37°C for 15 min. At the end of the incubation period, 300 μl of the mixture was put into an ESR tube and frozen in liquid nitrogen, and the ESR signal was measured at 77 K. Before incubation, 300 μl of the mixture was collected as a zero time control (22). As an untreated control, isolation medium was added instead of rotenone solution.

Effect of NADH Concentration on the Reduction of Cu-ATSM. A 0.8-ml aliquot of the SMP preparation was mixed with 0.1 ml of NADH solution and 0.1 ml of Cu-ATSM solution (0.2 mM) and then incubated at 37°C for 15 min. After incubation, the ESR signal was measured at 77 K. An aliquot of the mixture before incubation

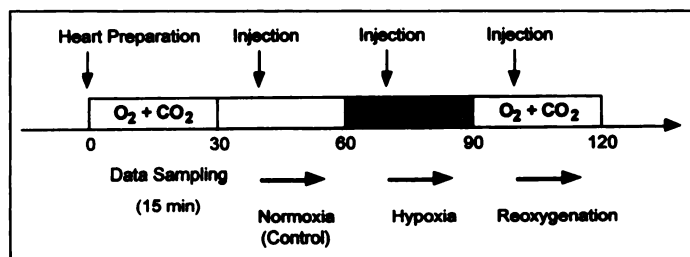


FIGURE 2. Experimental protocol for Langendorff rat perfused isolated heart model study.

was retained as a control. NADH solution was added at a concentration of 0 (isolation medium), 5 or 10 mM.

Preparation of Copper-62-ATSM and Copper-62-PTSM

[⁶²Cu]Cu-ATSM and [⁶²Cu]Cu-PTSM were prepared using the previously reported method (18). Briefly, 4 ml of ⁶²Cu-glycine solution obtained from the generator was mixed with 0.2 ml of ATSM or PTSM solution (0.4 and 2 mM in dimethyl sulfoxide, respectively). Radiochemical purity was more than 95%, as determined by reversed phase high performance liquid chromatography.

Mouse Biodistribution Studies

Male ddY mice weighing 25 g were injected with ⁶²Cu-ATSM or ⁶²Cu-PTSM solution (~740 kBq in 0.1 ml) via the tail vein. Mice were killed by ether anesthesia 1, 5 or 30 min after injection. Blood was collected by cardiac puncture using a syringe, and then the brain and heart were weighed. Copper-62 radioactivity was measured in a well-type scintillation counter (ARC-350, Aloka, Japan) with decay correction. Relative accumulation was calculated as percent dose/g of tissue.

Perfused Rat Heart Model Studies

The perfused rat heart model was prepared by a modification of the method of Langendorff (31). Male Wistar rats weighing 350–450 g were injected intraperitoneally with 500 IU of heparin 20 min before the hearts were isolated. Rats were stunned with a blow to the head; hearts were then quickly placed into cold perfusate and washed. The aortas were attached to a stainless steel cannula, and the hearts were retrogradely perfused at a rate of 6 ml/min at 37°C without recirculation. The perfusate used was a Krebs-Ringer's bicarbonate buffer, containing 118.5 mM NaCl, 4.6 mM KCl, 1.2 mM MgCl₂, 2.5 mM CaCl₂, 1.2 mM KH₂PO₄, 25.0 mM Na₂CO₃ and 12.8 mM glucose, continuously bubbled with 95% O₂ – 5% CO₂ or 95% N₂ – 5% CO₂ (pH 7.4).

The hearts were perfused with the oxygenated buffer for 30 min before use for the experiments. Normoxic buffer perfusion was performed for 30 min, and then perfusate was switched to nitrogenated buffer (hypoxia perfusion) for 30 min, followed by reoxygenated perfusion for 30 min. Tracer injections were performed with a six-direction valve injector 5 min after commencement of normoxic perfusion, hypoxic perfusion and reoxygenated perfusion, as shown in Figure 2. Radioactivity in the perfused heart was detected with a lead-shielded BGO detector and stored in a microcomputer. Background and decay correction of the data were performed as follows. Before the study, system background (SB, constant) was measured. Just before each ⁶²Cu-ATSM injection, apparent background data were obtained (apparent background at time 0, AB₀) that were considered as sums of SB and retained ⁶²Cu radioactivity originated from the previous injection (for first injection, AB₀ = SB). From the apparent radioactivity curve (AR_t), the true accumulation curve (TR_t) was obtained as follows:

$$\begin{aligned} TR_t &= (AR_t - SB)_{\text{decay corrected}} - (AB_t - SB)_{\text{decay corrected}} \\ &= (AR_t - SB)_{\text{decay corrected}} - (AB_0 - SB). \quad \text{Eq. 1} \end{aligned}$$

This calculation could be done because preliminary study indicated that washout of ⁶²Cu from the heart was completed by 10 min after injection under either normoxic or hypoxic conditions. Retention % was calculated based on the peak radioactivity in the heart as follows:

Retention % at time t

$$= \frac{TR_t}{\text{Peak TR found just after injection}} \times 100. \quad \text{Eq. 2}$$

In Vivo Left Anterior Descending (LAD) Coronary Artery Occluded Rat Heart Model Studies

LAD coronary artery occluded rat heart model was prepared as described previously (32). Male Wistar rats weighing 250 g were anesthetized with pentobarbital administered intraperitoneally. Animals were intubated and ventilated with room air with a rodent respirator (Natsume, Japan). Left thoracotomy was performed at the fourth intercostal space; the pericardium was opened, and a single fixed ligature was used to occlude flow of the LAD coronary artery with 6-0 vicryl. The thorax was closed, and after 30 min ⁶²Cu-ATSM and ²⁰¹Tl were co-injected (⁶²Cu: 500 μCi; ²⁰¹Tl: 5 μCi, in 0.5 ml saline) through the femoral vein. Rats were killed with an overdose of ether 10 min after tracer injection. Blood was collected by heart puncture with a heparinized syringe, and then the heart was removed and divided into 10–16 segments. Each segment was weighed, and ⁶²Cu radioactivity in each sample and blood was measured immediately with a well-type scintillation counter (energy window: 450–550 keV). Under these conditions, cross-talk from the ²⁰¹Tl to ⁶²Cu channel was negligible. Several hours later, i.e., after ⁶²Cu radioactivity had decayed out, ²⁰¹Tl radioactivity (energy window: 100–180 keV) was measured. Relative accumulation of both ⁶²Cu and ²⁰¹Tl in each segment was calculated as tissue-to-blood ratio of percent dose/g.

Protein Assay

Each sample was diluted with 1% sodium dodecyl sulfate, and the protein concentration was measured using a BCA protein assay reagent.

ESR Spectrometry

ESR spectra of Cu-ATSM were determined with an X-band spectrometer. Spectrometry conditions were 5 mW microwave power, 6.3 gauss modulation amplitude, 100 kHz modulation frequency and 9.25 GHz microwave frequency with a magnetic field of 2800–3800 gauss at 77 K.

Electrochemistry

Half-wave potentials, as redox potentials, were measured at room temperature (~25°C) in a stirred solution of 55% dimethyl sulfoxide + 45% HEPES buffer (50 mM, pH 7.4), using platinum as the working electrode and a saturated calomel electrode as the reference. Redox potential of Cu-ATSM was corrected to the known redox potential of Cu-PTSM (21) as a standard. Single sweep voltammetry was performed with a polarographic analyzer.

Statistical Analysis

Unpaired alternate Welch Student's t-test was used for statistical analysis.

RESULTS

Redox Potential of Cu-ATSM

The redox potential of Cu-PTSM was reported to be –208 mV (21), which is rather high when compared with that of NADH [–315 mV, (33)]. In this study, Cu-ATSM showed a redox potential of –297 mV, lower than that of Cu-PTSM, but similar to that of NADH.

TABLE 1
Biodistributions of Copper-62-ATSM and Copper-62-PTSM in Mice

| Tissue | Time after injection (min) | | |
|-----------------------------|----------------------------|--------------|--------------------------|
| | 1 | 5 | 30 |
| ⁶²Cu-ATSM | | | |
| Blood | 3.04 (0.14) | 2.37 (0.21) | 2.08 (0.19) |
| Brain | 7.24 (0.12) | 3.52 (0.14) | 2.50 (0.15) |
| Heart | 6.80 (0.09) | 3.05 (0.29) | 2.43 (0.17) |
| Brain/blood | 2.39 (0.07) | 1.49 (0.11)* | 1.21 (0.18)* |
| Heart/blood | 2.24 (0.13) | 1.30 (0.21)* | 1.17 (0.08)* |
| ⁶²Cu-PTSM | | | |
| Blood | 4.01 (0.27) | 2.73 (0.27) | 0.82 (0.71) |
| Brain | 8.23 (1.37) | 7.15 (0.56) | 7.42 (1.01) |
| Heart | 21.64 (7.25) | 14.94 (1.39) | 14.62 (2.69) |
| Brain/blood | 2.05 (0.29) | 2.64 (0.37) | 4.73 (0.40) [†] |
| Heart/blood | 5.36 (1.57) | 5.53 (0.99) | 8.42 (1.43) [‡] |

*Significantly low when compared with 1-min value ($p < 0.0001$).

[†]Significantly high when compared with 1-min value ($p < 0.0001$).

[‡]Significantly high when compared with 1-min value ($p < 0.01$).

Effect of Rotenone Treatment on Mitochondrial Reduction of Cu-ATSM

The effects of disturbed electron flow in the electron transport chain on the mitochondrial reduction of Cu-ATSM were studied using rotenone as an inhibitor of Complex I. With nontreated control mitochondria, only a reduction of 3.4% (2.7%) (average (1 s.d.) of four experiments) was observed, but rotenone treatment significantly increased the reduction to 14.7% (3.4%) (average (1 s.d.) of four experiments), 4-fold higher than that of the control ($p < 0.01$, when compared with the control).

Effects of NADH Concentration on the Reduction of Cu-ATSM by SMP

The reduction of Cu-ATSM by SMP was NADH-dependent; i.e., 2.7% (1.3%), 21.6% (6.7%) and 29.0% (7.1%) (average (1 s.d.) of four experiments), when exogenous NADH was added at 0, 500 and 1000 μM , respectively. However, reduction of Cu-ATSM required a larger dose when compared with Cu-PTSM reduction (22). Cu-ATSM could not be reduced by NADH alone.

Mouse Biodistribution Studies

Table 1 shows the biodistributions of ⁶²Cu-ATSM and ⁶²Cu-PTSM in mice. As reported previously, ⁶²Cu-PTSM showed high retention in the brain as well as the heart. As a result, brain to blood ratios (B/B) as well as heart to blood ratios (H/B) increased with time after injection. Copper-62-ATSM also showed high brain and heart uptake just after injection but was quickly washed out from these tissues. Consequently, B/B and H/B were significantly decreased and reached values of 1.

Perfused Rat Heart Model Studies

Typical retention profiles of ⁶²Cu-ATSM in isolated perfused heart preparations under conditions of normoxia, hypoxia and reoxygenation are shown in Figure 3. Average retention % values (1 s.d.) of five different heart preparations under normoxic, hypoxic and reoxygenated conditions at 15 min after injection were 23.77 (2.98), 81.10 (3.41), ($p < 0.0001$ when compared with normoxia) and 22.80 (4.75), respectively. Under normoxic as well as reoxygenated conditions, only 20% of the ⁶²Cu-ATSM injected as a bolus was retained in the heart, and 80% was quickly washed out. In the same heart preparations,

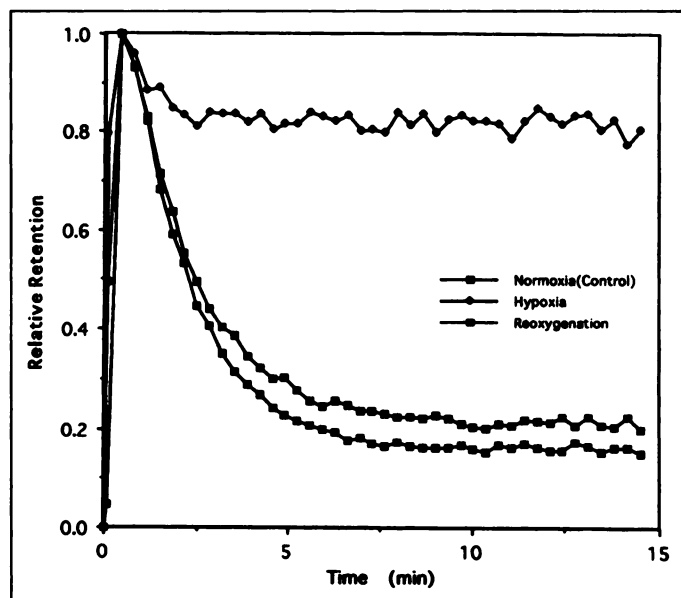


FIGURE 3. Typical retention profiles of ⁶²Cu-ATSM in Langendorff rat perfused isolated hearts under normoxic, hypoxic and reoxygenated conditions.

however, more than 80% of the injected ⁶²Cu-ATSM was retained under hypoxic condition.

In Vivo LAD Occluded Rat Heart Model Studies

Relative ⁶²Cu-ATSM accumulation in various segments of four LAD occluded rat hearts is plotted in Figure 4 with relative ²⁰¹Tl accumulation in the corresponding segments. Copper-62 radioactivity accumulation increased with the decrement of ²⁰¹Tl accumulation, an index of relative myocardial perfusion. In the segments of severely low ²⁰¹Tl accumulation, ⁶²Cu accumulation was also decreased.

DISCUSSION

Compounds known as hypoxic sensitizers, of which nitroimidazole is an example, are localized within hypoxic but nonnecrotic tumor cells (34). Interestingly, copper itself has also been reported to be a hypoxic cell sensitizer, and its redox reaction is closely correlated with cell toxicity (35). Thus, it is reasonable

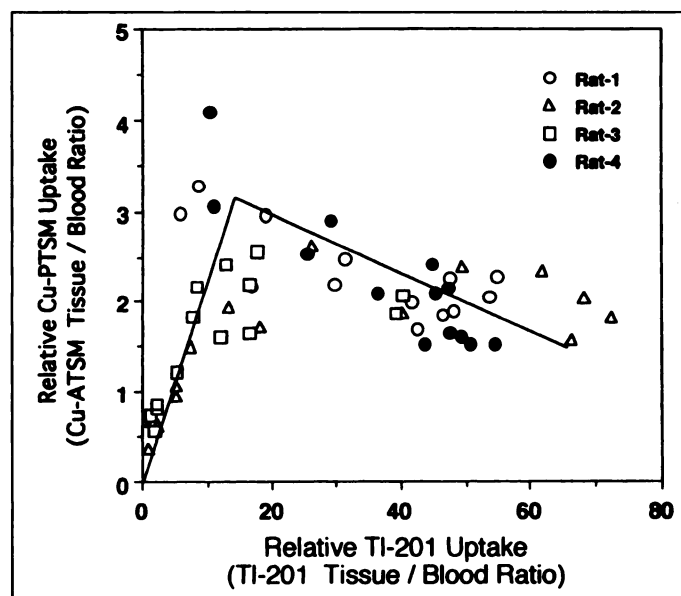


FIGURE 4. Relationship between the myocardial accumulation of ⁶²Cu-ATSM and ²⁰¹Tl 10 min after intravenous injection.

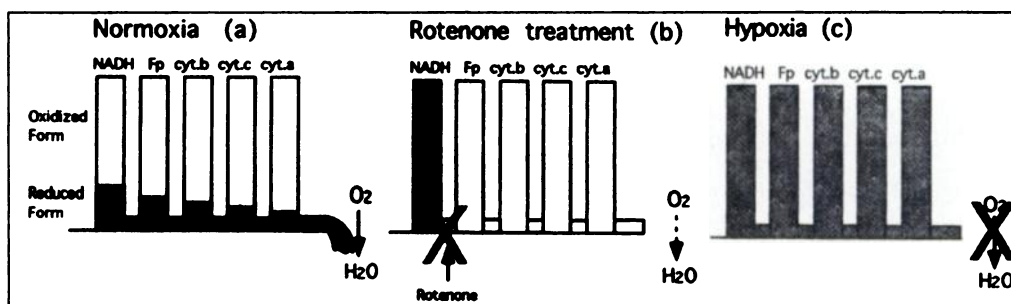


FIGURE 5. Schematic water pressure model of electron transport chain under normoxia (a), rotenone treatment (b) and reoxygenation conditions (c).

to screen for new hypoxia imaging agents among copper complexes.

As essential characteristics for hypoxia imaging agents, a candidate should have small molecular size as well as suitable lipophilicity for easy penetration through the cell membranes, including the blood-brain barrier. It has been reported that various radiolabeled Cu-BTS complexes efficiently cross the blood-brain barrier (23). In the present mouse biodistribution study, ^{62}Cu -ATSM showed quick penetration into both the brain and the heart. This characteristic enables access to the oxygen-depleted mitochondria in hypoxic cells.

Cu-ATSM had the same range of redox potential as NADH, which was about 100 mV lower than that of Cu-PTSM. Previously, we showed that Cu-PTSM is reduced at Complex I site of electron transport chain using NADH as an electron donor (22). Under the same conditions, Cu-ATSM was less reduced by normal electron transport chain, probably because of its low redox potential. As a result, ^{62}Cu -ATSM showed high access into normal tissues but quick washout.

However, in the rotenone-treated mitochondria, Cu-ATSM reduction was increased to four times the value under basal conditions. Rotenone disturbs electron flow between Complex I and ubiquinone (Fig. 5b). This is considered to be comparable with hypoxia, i.e., hyper-reduction of Complex I caused by depletion of oxygen, the final electron acceptor (Fig. 5c). Similar results were also observed in NADH-loaded SMP. SMP preparations lost endogenous NADH and could not reduce Cu-ATSM. However, Cu-ATSM reduction occurred when a sufficient dose of NADH was added to the reaction medium. NADH concentration is known to increase in hypoxic tissues (36), and Cu-ATSM might be reduced in such segments.

Based on the results of *in vitro* studies, hypoxia-selective retention of ^{62}Cu -ATSM was studied using Langendorff isolated perfused rat hearts. In this model, oxygen concentration can be controlled without any change in flow rate or substrate supply. In this study, ^{62}Cu -ATSM showed a very high degree of hypoxia-selective retention when injected as a bolus into the heart preparations. This was partly because of the ease of entry

of ^{62}Cu -ATSM into the cells and partly due to the selective affinity to Complex I with abnormally high electron and/or NADH concentrations. In addition, serial studies using the same preparations demonstrated that hypoxic retention of ^{62}Cu -ATSM was a reversible phenomenon. Thus, the retention of ^{62}Cu -ATSM was dependent only on oxygen concentration and not on hypoxia-related long-lasting changes such as membrane damage.

In the LAD-occluded rat heart model, tissue segments with various ^{201}Tl uptake levels could be obtained. In the Langendorff perfused rat heart model, 30-min complete ischemia did not induce crucial damage in heart function (37). Thus, at this time point, i.e., just after 30-min occlusion, myocardium was considered to be still viable, and ^{201}Tl accumulation could be evaluated as relative perfusion levels of the tissue. As ^{201}Tl accumulation decreased, ^{62}Cu accumulation was gradually increased, and tissue-to-blood ratio reached approximately 2.5. Within this range, ^{62}Cu accumulation seemed to be inversely proportional to the ^{201}Tl accumulation, possibly blood flow levels, of the corresponding segment. However, in segments with no or extremely low ^{201}Tl accumulation, ^{62}Cu accumulation was proportional to it. In these segments, the reduction ability of electron transport chain for ^{62}Cu -ATSM was considered to be maximal, and restricted supply of ^{62}Cu became a determinant of ^{62}Cu retention. Decrements of ^{62}Cu accumulation, however, were found in two rats, but not in others. The preparation of this infarction model was not well controlled so that size of the infarcted area varied in each animal. As a result, these two rats might have had incomplete ischemia, lacking severely suppressed flow. However, further autoradiographic studies using other radioactive copper nuclides with longer half-lives in combination with histological analysis are needed to confirm this consideration.

This study indicated that ^{62}Cu -ATSM accumulates in the hypoxic myocardium by a reductive retention mechanism by mitochondria with disturbed electron flow, and this effect is independent of flow. Rapid washout from the other tissues including normal myocardium as well as favorable blood-pool clearance may allow rapid identification of patients with myocardial hypoxia. As shown in Figure 6, the proposed retention mechanism of this compound was very simple and might be applied to other pathological states such as brain ischemia, tumors, etc. Further studies are currently in progress to clarify the actual retention mechanisms of these target tissues. The proposed criteria for hypoxic imaging agents might not be satisfied only by Cu-ATSM but other Cu complexes as well as other metallic/organic compounds. Some Cu complexes with and without BTS structure were examined, and some encouraging results were obtained (to be published elsewhere).

Combination of generator-produced ^{62}Cu and the simple labeling procedure using kits will permit on-demand supply of the radiopharmaceutical for patients with acute ischemic insults, and it

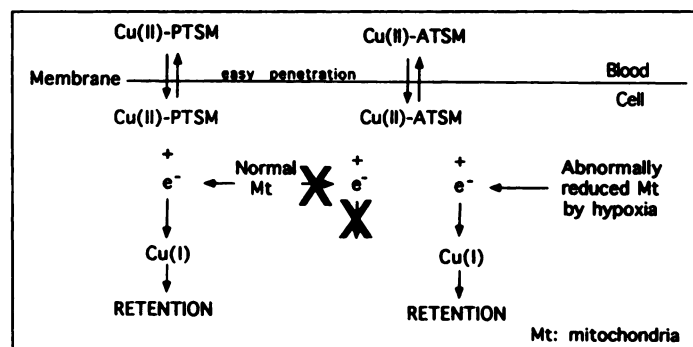


FIGURE 6. Estimated mechanism of retention of ^{62}Cu -ATSM as a hypoxic imaging agent.

might provide new pathophysiological information for understanding the mechanism of cell damage in ischemic diseases.

ACKNOWLEDGMENT

We thank Nihon Medi-Physics Co. Ltd, Japan, for supplying ^{62}Zn and ^{201}Tl .

REFERENCES

1. Adams GE, Flockhart IR, Smithen CE, et al. Electron-affinic sensitization VII. A correlation between structures, one-electron reduction potentials and efficiencies of nitroimidazoles as hypoxic cell radiosensitizers. *Radiat Res* 1976;67:9–20.
2. Chapman JD, Baer K, Lee J. Characteristics of the metabolism-induced binding of misonidazole to hypoxic mammalian cells. *Cancer Res* 1983;43:1523–1528.
3. Hoffman JM, Rasey JS, Spence AM, et al. Binding of the hypoxia tracer [^3H]misonidazole in cerebral ischemia. *Stroke* 1987;18:168–176.
4. Jerabek PA, Patrick TB, Kilbourn MR, et al. Synthesis and biodistribution of ^{18}F -labeled fluoronitroimidazoles: potential in vivo markers of hypoxic tissue. *Int J Radiat App Instrum [A]* 1986;37:599–605.
5. Parliament MB, Chapman JD, Urtasun RC, et al. Non-invasive assessment of human tumor hypoxia with ^{123}I -iodoazomycin arabinoside: preliminary report of a clinical study. *Br J Cancer* 1992;65:90–95.
6. Mannan RH, Mercer JR, Wiebe LI, et al. Radioiodinated 1-(2-fluoro-4-iodo-2,4-dideoxy-beta-L-xylopyranosyl)-2-nitroimidazole: a novel probe for the noninvasive assessment of tumor hypoxia. *Radiat Res* 1992;132:368–374.
7. Linder KE, Chan YW, Cyr JE, et al. Technetium-O(PnAO-(2-nitroimidazole)) [BMS181321], a new technetium-containing nitroimidazole complex for imaging hypoxia: synthesis characterization and xanthine oxidase-catalyzed reduction. *J Med Chem* 1994;37:9–17.
8. Linder KE, Chan YW, Cyr JE, et al. Synthesis, characterization and in vitro evaluation of nitroimidazole-BATO complexes: new technetium compounds designed for imaging hypoxic tissue. *Bioconjug Chem* 1993;4:326–333.
9. Brown JM, Workman P. Partition coefficient as a guide to the development of radiosensitizers which are less toxic than misonidazole. *Radiat Res* 1980;82:171–190.
10. Ng CK, Sinusas AJ, Zaret BL, Soufer R. Kinetic analysis of technetium-99m-labeled nitroimidazole (BMS-181321) as a tracer of myocardial hypoxia. *Circulation* 1995;92:1261–1268.
11. Nunn A, Linder K, Strauss HW. Nitroimidazoles and imaging hypoxia. *Eur J Nucl Med* 1995;22:265–280.
12. Rumsey WL, Patel B, Linder KE. Effect of graded hypoxia on retention of technetium-99m-nitroheterocycle in perfused rat heart. *J Nucl Med* 1995;36:632–636.
13. Hall EJ. Radiosensitizers and bioreductive drugs. In: *Radiology for the radiologist*, 4th ed. Philadelphia, PA: JB Lippincott; 1994:165–181.
14. Aboagye EO, Lewis AD, Johnson A, et al. The novel fluorinated 2-nitroimidazole hypoxia probe SR-4554: reductive metabolism and semiquantitative localization in human ovarian cancer multicellular spheroids as measured by electron energy loss spectroscopic analysis. *Br J Cancer* 1995;72:312–318.
15. Hearse DJ, Manning AS, Downey JM, Yellon DM. Xanthine oxidase: a critical mediator of myocardial injury during ischemia and reperfusion. *Acta Physiol Scand* 1986;548(suppl):65–78.
16. McGilvery RW, Goldstein GW. Turnover of nucleotides. In: *Biochemistry, a functional approach*, 3rd ed. Philadelphia, PA: WB Saunders; 1983:675–696.
17. Fujibayashi Y, Matsumoto K, Yonekura Y, et al. A new zinc-62/copper-62 generator as a copper-62 source for PET radiopharmaceuticals. *J Nucl Med* 1989;30:1838–1842.
18. Matsumoto K, Fujibayashi Y, Yonekura Y. Application of the new zinc-62/copper-62 generator: an effective labeling method for ^{62}Cu -PTSM. *Nucl Med Biol* 1992;19:39–44.
19. Okazawa H, Yonekura Y, Fujibayashi Y, et al. Measurement of segmental cerebral plasma pool and hematocrit with ^{62}Cu -labeled HSA-DTS. *J Nucl Med* 1997;in press.
20. Fujibayashi Y, Taniuchi H, Wada K, et al. Differential mechanism of retention of Cu-pyruvaldehyde-bis(N^4 -methylthiosemicarbazone) (Cu-PTSM) by brain and tumor: a novel radiopharmaceutical for positron emission tomography imaging. *Ann Nuklearmedizin* 1995;9:1–5.
21. Minkel DT, Saryan LA, Petering DH. Structure-function correlations in the reaction of bis(thiosemicarbazonato) copper(II) complexes with Ehrlich ascites tumor cells. *Cancer Res* 1978;38:124–129.
22. Taniuchi H, Fujibayashi Y, Okazawa H, et al. Cu-pyruvaldehyde-bis(N^4 -methylthiosemicarbazone) (Cu-PTSM), a metal complex with selective NADH-dependent reduction by Complex I in brain mitochondria; a potential radiopharmaceutical for mitochondria-functional imaging with positron emission tomography. *Biol Pharm Bull* 1995;18:1126–1129.
23. John EK, Green MA. Structure-activity relationships for metal-labeled blood flow tracers: comparison of keto aldehyde bis(thiosemicarbazonato) copper(II) derivatives. *J Med Chem* 1990;33:1764–1770.
24. Archer CM, Edwards B, Kelly JD, et al. Technetium-labeled agents for imaging tissue hypoxia in vivo. In: Nicolini M, Bandoli G, Mazzi U, eds. *Technetium and rhenium in chemistry and nuclear medicine 4*. Padova, Italy: SGE Ditoriali; 1995:535–549.
25. Gingas BA, Suprunchuk T, Bayley CH. The preparation of some thiosemicarbazones and their copper complexes. Part III. *Can J Chem* 1962;40:1053–1059.
26. Higuti T, Arakaki N, Niimi S, et al. Anisotropic inhibition of energy transduction in oxidative phosphorylation in rat liver mitochondria by tetraphenylarsonium. *J Biol Chem* 1980;255:7631–7636.
27. Williams N, Amzel LM, Pedersen PL. Proton ATPase of rat liver mitochondria: a rapid procedure for purification of stable, reconstitutively active F_1 preparation using a modified chloroform method. *Anal Biochem* 1984;140:581–588.
28. Ohmomo Y, Hirata M, Murakami K, et al. Synthesis of fluorine and iodine analogs of clorgyline and selective inhibition of monoamine oxidase A. *Chem Pharm Bull* 1991;39:1038–1040.
29. Pennington RJ. Biochemistry of dystrophic muscle. Mitochondrial succinate-tetrazolium reductase and adenosine triphosphatase. *Biochem J* 1961;80:649–654.
30. Ochoa S. Malic dehydrogenase from pig heart. *Methods Enzymol* 1955;1:735–739.
31. Sakai K, Shiraki Y. A device for recording left ventricular contraction and electrocardiogram in nonworking isolated perfused rat heart. *Jpn J Pharmacol* 1978;28:223–229.
32. Ohtani H, Callahan RJ, Khaw BA, et al. Comparison of technetium-99m-glucuronate and thallium-201 for the identification of acute myocardial infarction in rats. *J Nucl Med* 1992;33:1988–1993.
33. McGilvery RW, Goldstein GW. Oxidations and phosphorylations. In: *Biochemistry, a functional approach*, 3rd ed. Philadelphia, PA: WB Saunders; 1983:390–420.
34. Shelton ME, Dence CS, Hwang DR, et al. Myocardial kinetics of fluorine-18 misonidazole: a marker of hypoxic myocardium. *J Nucl Med* 1989;30:351–358.
35. Hesselwood IP, Cramp WA, McBrien DCH, et al. Copper as a hypoxic cell sensitizer of mammalian cells. *Br J Cancer* 1978;37(suppl):95–97.
36. Barlow CH, Harken AH, Chance B. Evaluation of cardiac ischemia by NADH fluorescence photography. *Ann Surg* 1977;186:737–740.
37. Wada K, Fujibayashi Y, Taniuchi H, et al. Effects of ischemia-reperfusion injury on myocardial single pass extraction and retention of Cu-PTSM in perfused rat hearts: comparison with ^{201}Tl and ^{14}C -iodoantipyrine. *Nucl Med Biol* 1994;21:613–617.